

# Generating Schrodinger-cat states in momentum and internal-state space from Bose-Einstein condensates with repulsive interactions

J. Higbie and D. M. Stamper-Kum

Department of Physics, University of California, Berkeley CA 94720

(Dated: March 22, 2024)

Resonant Raman coupling between internal levels induced by continuous illumination of non-collinear laser beams can create double-well momentum-space potentials for multi-level "periodically-dressed" atoms. We develop an approximate many-body formalism for a weakly interacting, trapped periodically-dressed Bose gas which illustrates how a tunable exchange interaction yields correlated many-body ground states. In contrast to the case of a position-space double well, the ground state of stable periodically-dressed Bose gases with repulsive interactions tends toward a Schrodinger cat state in the regime where interactions dominate the momentum-space tunnelling induced by the external trapping potential. The dependence of the momentum-space tunnelling and exchange interaction on experimental parameters is derived. We discuss how real-time control of experimental parameters can be used to create Schrodinger cat states either between momentum or internal states, and how these states could be dynamically controlled towards highly sensitive interferometry and frequency metrology.

PACS numbers: 03.75.Gg, 05.30.Jp, 52.38.Bv

Following our mastery over the internal and external states of individual atoms, the scientific frontier advances to the full control over the quantum states of many-body systems. Entangled states, in which the constituents of a many-body system display non-classical correlations, play a key role in our developing understanding of quantum information and decoherence, and may find practical use in quantum communication [1], quantum computing, and high-precision metrology [2, 3, 4, 5]. Various techniques are being developed that generate entanglement deterministically in, for example, spin-squeezed atomic ensembles [6], trapped ions [7], the electromagnetic field [8], and superconducting circuits [9, 10].

Ultracold neutral atoms offer a promising route to generating highly entangled many-body states. Schemes for generating such entanglement rely on interatomic interactions which provide "non-linear" elements as seen from the viewpoint of single-particle dynamics. Such non-linear terms are provided naturally through binary collisions between ground-state atoms, as utilized controllably by Mandel et al. [11], and can be further enhanced through molecular resonances or by the assistance of near-resonant photons [12, 13].

A paradigmatic system in which interatomic interactions induce entanglement is a collection of ultracold interacting bosons in a parity-symmetric double-well potential [14, 15, 16, 17]. The lowest-energy single-particle states are the parity-even ground state  $|j_0\rangle$  and parity-odd first excited state  $|j_1\rangle$ , separated in energy by the tunnel splitting  $J$ . If tunnelling and interactions are weak with respect to the energy spacings to other single-particle states, the many-body system may be described by the two-mode Hamiltonian

$$H = \frac{J}{2} \hat{c}_R^\dagger \hat{c}_L + \hat{c}_L^\dagger \hat{c}_R + U \hat{N}_R \hat{N}_L \quad (1)$$

whence terms dependent only on the total number of atoms in the system are omitted. Here  $\hat{c}_R$  and  $\hat{c}_L$  denote

annihilation operators for particles in the right- ( $\hat{c}_R = |j_0\rangle\langle j_1| = \sqrt{2}$ ) or left- ( $\hat{c}_L = |j_1\rangle\langle j_0| = \sqrt{2}$ ) well states, respectively. The number operators  $\hat{N}_R = \hat{c}_R^\dagger \hat{c}_R$  and  $\hat{N}_L = \hat{c}_L^\dagger \hat{c}_L$  count particles in the right or left wells, respectively, of the double-well system. The parameter  $U$  gives the energy due to short-range interactions of a pair of atoms located in the same well.

This simple Hamiltonian leads to highly-correlated many-body ground states through the interplay of tunnelling and interaction. One finds three limiting behaviors. If the tunneling rate dominates, the many-body ground-state of  $N$  bosons is driven to the factorized, uncorrelated state in which all  $N$  atoms are identically in the single-particle ground state  $|j_0\rangle$ . In the limit  $N \gg J/U$ , the interaction energy dominates. For repulsive interactions ( $U > 0$ ), a many-body state divides itself evenly between the two potential minima, generating the state  $|j_0\rangle / (\hat{c}_R^\dagger)^N = 2^{-N/2} (\hat{c}_L^\dagger)^N |j_0\rangle$ , where  $|j_0\rangle$  is the vacuum state. Experimental evidence for such a "number-squeezed" state has been obtained by Orzel et al. in a many-well potential [18]. Similar physics is responsible for the observed Mott-insulator phase in a three-dimensional periodic potential [19].

For attractive interactions ( $U < 0$ ), the ground-state is quite spectacular: a Schrodinger-cat state  $|j_0\rangle / [(\hat{c}_R^\dagger)^N + (\hat{c}_L^\dagger)^N] |j_0\rangle$  formed as a superposition of states in which all atoms are found in one of the two wells. The generation of Schrodinger cat states is a tantalizing goal; at present, the largest atomic Schrodinger-cat states contain just four atoms [7]. However, accomplishing this goal by imposing a double-well potential on a collection of bosons with attractive interactions is a daunting task: such Bose-Einstein condensates are unstable to collapse [20], implying that the number of bosons placed into the superposition state will be small; moreover, exceptional spatial control over trapping potentials and over the in-

interaction strength is required.

The above discussion pertains to atoms for which the position-space potential is a double well, while the kinetic energy term  $p^2/2m$  may be regarded as a momentum-space harmonic "potential." In this work, we point out that an analogous many-body system can be crafted, in which the roles of position and momentum are interchanged. As discussed in previous work [21, 22, 23], the dispersion relation of multi-level atoms placed in a spatially-periodic coupling between internal states can take the form of a momentum-space double-well "potential." Addition of an harmonic position-space trapping potential produces a double-well system dual to that discussed above. Assessing the roles of interparticle interactions in this situation, we find that the many-body ground states for bosonic atoms in such a system are highly-entangled in both momentum- and internal-state space. In opposition to the situation of bosons in position-space double wells, maximally-entangled states may be generated in the case of repulsive interactions, allowing the creation of such states starting with large, stable Bose-Einstein condensates while obviating the need for exacting control over potentials with extremely small spatial dimensions.

The roles of repulsive or attractive interactions in determining the behaviour of interacting bosons in momentum-space double-well potentials are reversed from those in the case of position-space potentials. As discussed below, this reversal is due to an exchange term which arises in the evaluation of the interaction energy of a Bose gas that occupies several distinct momentum states. For repulsive interactions, for example, this exchange term disfavors a macroscopic occupation of more than one single-particle wavefunction (the so-called fractionation of a condensate as discussed by Leggett [24] and others), thus favoring a Schrodinger-cat superposition. We find that the strength of the exchange term can be dynamically varied by varying parameters of the periodic coupling field which generates the double-well potential.

Following a derivation of the momentum-space double-well potential (Sec. I), we develop a two-mode approximate treatment of this system which provides expressions for the interaction and tunnelling energies and thereby clarifies their dependence on experimental parameters (Sec. II). Similar work by Arecchi and Montina [23] treats this system using the Gross-Pitaevskii equation as the starting point, a numerical scheme which identifies the onset of correlated many-body ground states. Their work appears to reproduce our analytic approach in the limit of weak interactions, while the validity of their approach (or, indeed, any extant treatment) for stronger interactions is difficult to establish. Furthermore, in Section III, we show that maximally-entangled states can be generated purely between internal states or between momentum states, offering a route to Heisenberg-limited atomic clocks [3] or atomic interferometry [5], respectively.

## I. ORIGIN OF THE MOMENTUM-SPACE POTENTIAL

We consider bosonic atoms of mass  $m$  with two internal states,  $|A\rangle$  and  $|B\rangle$ , at energies  $\sim \epsilon_A$  and  $\sim \epsilon_B$ , respectively. These atoms are exposed to laser fields of frequencies  $\omega_1$  and  $\omega_2$  ( $\omega = \omega_1 - \omega_2$ ) and wavevectors  $k_1$  and  $k_2$  which induce Raman transitions between the two internal states (see Fig. 1a,b). Thus, a Raman process from state  $|A\rangle$  to  $|B\rangle$  imparts a momentum of  $\hbar k = \hbar(k_1 - k_2)$  and kinetic energy of  $\sim \epsilon_B - \epsilon_A$ . The continuous Raman coupling can be regarded as a spatially-periodic coupling field between the internal states of the atoms, represented by an off-diagonal potential  $V_R = \frac{\hbar\Omega}{2} e^{i(k \cdot r - \omega t)} |A\rangle\langle B| + e^{i(k \cdot r + \omega t)} |B\rangle\langle A|$ . Here  $\Omega$  is the two-photon Rabi frequency, taken to be real, which is determined by dipole matrix elements, the detuning from intermediate resonances, and by the laser intensities.

It is convenient to analyze this constantly-driven system in terms of "periodically-dressed" states, which are coherent superpositions of both internal and external (momentum) states. As developed in Refs. [21, 22], this treatment reveals marked anisotropy and tunability in the superfluid characteristics of a Bose-Einstein condensate formed of such a dressed-state gas. Given a two-component spinor wavefunction  $\tilde{\psi}(r) = (\psi_A(r); \psi_B(r))$  to describe single-atom states in the  $|A\rangle, |B\rangle$  basis, we transform to a frame which is co-rotating and co-moving with the driving laser fields, yielding a spinor wavefunction  $\tilde{\psi}(r)$  with components  $\psi_{A,B}(r) = \exp(-i(k \cdot r - \omega t)/2) \psi_{A,B}(r)$ . This transformation yields a Schrodinger equation with two deBroglie wave solutions at each momentum  $\hbar q$ , which we call the periodically-dressed states. The two-branch dispersion relation of the periodically-dressed atoms has the form (using  $\hbar$  for plus and minus)

$$\epsilon_{\pm}(q) = \epsilon_B + \frac{1}{4} \frac{1}{2} \frac{\Omega^2}{(2q - k)^2 + \omega^2} \quad (2)$$

where energies and wavevectors are scaled by the Raman recoil energy  $E_k = \hbar^2 k^2 / 2m$  and wavevector  $k$ , respectively.

Under the conditions of exact Raman resonance ( $\omega = 0$ ) and sufficiently small Rabi frequency  $\Omega$ , a degeneracy of momentum ground states occurs as the lower dispersion relation takes the form of a double-well potential, with minima at  $Q = 2(Q \pm k)$  (Fig. 1c). This potential can be quickly tuned by modifying the laser based parameters. The detuning from Raman resonance breaks the ground-state degeneracy, favoring the right- or left-well states. The spacing between the potential wells is controlled by the Raman momentum transfer  $\hbar k$ , which can be varied by reorienting the laser beams. Finally, the Rabi frequency  $\Omega$  changes both the height of the barrier between the wells, as well as the internal-state character of states on either side of the well [22].

In the case of a position-space double well, the kinetic energy of the atoms forbids a complete localization of

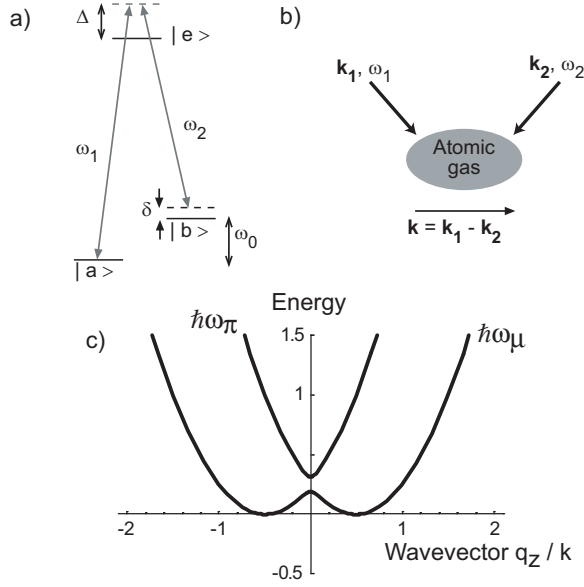


FIG. 1: Creating a double-well momentum-space potential with Raman excitation. (a) Laser beams of frequency  $\omega_1$  and  $\omega_2$  may induce Raman transitions between internal states  $|a\rangle$  and  $|b\rangle$ .  $\delta = (\omega_1 - \omega_2) - \omega_0$  is the detuning from the Raman resonance. (b) Such a Raman transition in parts a momentum transfer of  $\sim k = k_1 - k_2$ , where  $k_1$  and  $k_2$  are the wavevectors of the Raman coupling lasers. (c) Atoms exposed to continuous Raman excitation can be described by a two-branch dispersion relation. Energies (scaled by  $E_k$ ) for the lower ( $\sim -$ ) and upper ( $\sim +$ ) dressed states are shown for wavevectors (scaled by  $k$ ) in the direction of the Raman momentum transfer. In the case of exact Raman resonance ( $\delta = 0$ ) and small Raman Rabi frequency (shown for  $\sim E_k = 1/8$ ), the lower dispersion relation takes the form of a parity-symmetry double-well potential.

atoms in either of the wells, thus introducing tunnelling. Similarly, in our case of the momentum-space double-well, a tunnelling between well-defined momentum states can be induced by adding a spatially-dependent term to the Hamiltonian. We consider adding an internal-state independent position-space trapping potential of the form  $V(x) = m \omega_x^2 x^2 / 2$  [25]. The Hamiltonian for this system may be written in the basis of the periodically-dressed states introduced earlier, using the expansion

$$\tilde{\psi}(x;t) = \sum_{\mathbf{q}} \frac{d^3 q}{(2\pi)^{3/2}} R(\mathbf{q}) \begin{pmatrix} \psi_-(\mathbf{q}) \\ \psi_+(\mathbf{q}) \end{pmatrix} e^{i\mathbf{q} \cdot \mathbf{r}} \quad (3)$$

where  $R(\mathbf{q}) = e^{i\mathbf{y} \cdot \mathbf{q}} / \sqrt{2}$  where  $\mathbf{y}$  is a Pauli matrix and the mixing angle  $\mathbf{q}$  is defined by the relation  $\cot \mathbf{q} = (\psi_+ / \psi_- - k/m) = \dots$ . The wavefunction  $\tilde{\psi}(\mathbf{q}) = (\psi_-(\mathbf{q}); \psi_+(\mathbf{q}))$  in the space of periodically-dressed momentum eigenstates obeys a Schrödinger equation with Hamiltonian

$$\hat{H}_{PD} = \begin{pmatrix} \sim \omega_+ & 0 \\ 0 & \sim \omega_- \end{pmatrix} + \frac{1}{M} \sum_{\mathbf{q}} R^y(\mathbf{q}) x_q^2 R(\mathbf{q}) \quad (4)$$

The position-space trapping potential is seen in momentum space as a kinetic-energy-like term (involving

$x_q^2$ ), which accounts also for the variations with  $q$  of the periodically-dressed eigenstate basis. The relevance of this kinetic-energy-like term is measured by the dimensionless effective mass parameter  $M$ , which is related to the Lamb-Dicke parameter  $\eta = \sqrt{m \omega_x / \hbar k}$  as  $M = 2 \eta^2$ . For weak spatial confinement ( $M \gg 1$ ), the low-energy single-particle states are restricted primarily to the lower periodically-dressed states, with the two lowest states split by a small tunnelling energy  $J$ . For strong confinement ( $M \ll 1$ ), the single-particle states are admixtures of upper- and lower-dispersion-periodically-dressed states, and a simple double-well treatment is no longer adequate.

To introduce interatomic interactions, we make use of the field operator  $\hat{\psi}(\mathbf{q}) = (\hat{\psi}_-(\mathbf{q}); \hat{\psi}_+(\mathbf{q}))$  the components of which annihilate particles in the lower ( $-$ ) or upper ( $+$ ) periodically-dressed states. These operators obey Bose commutation relations. We consider low-energy, binary, elastic collisions with a state-independent scattering length  $a$ . The interaction Hamiltonian then takes the form  $\hat{H}_{int} = \frac{g}{2} \int d^3 q \hat{\psi}^\dagger(\mathbf{q}) \hat{\psi}^\dagger(-\mathbf{q}) \hat{\psi}(\mathbf{q}) \hat{\psi}(-\mathbf{q})$ , neglecting terms dependent only on the total number of atoms  $N$ , where  $\hat{\psi}(\mathbf{q})$  is the spatial Fourier transform of the density operator, and  $g = 8 \pi \hbar^2 a$  is the properly scaled interaction parameter. The density operator is given as [21, 22]

$$\hat{n}(\mathbf{q}) = \sum_{\mathbf{q}'} \frac{d^3 q'}{(2\pi)^{3/2}} \hat{\psi}_-^\dagger(\mathbf{q} + \frac{\mathbf{q}'}{2}) R^y(\mathbf{q} + \frac{\mathbf{q}'}{2}) R(\mathbf{q} - \frac{\mathbf{q}'}{2}) \hat{\psi}_-(\frac{\mathbf{q}'}{2}) \quad (5)$$

## II. THE TWO MODE APPROXIMATION

To simplify our treatment, let us consider only the situation in which the two lowest energy eigenvalues (in the absence of interactions) are well separated from the remaining energies, and thus a two-mode description of the many-body system is adequate. The two lowest-energy single-particle states have wavefunctions  $\tilde{\psi}_0(\mathbf{q})$  and  $\tilde{\psi}_1(\mathbf{q})$ , mode operators  $\hat{c}_0$  and  $\hat{c}_1$ , and energy splitting  $J$ . We define the right- and left-well states as  $\tilde{\psi}_{R,L}(\mathbf{q}) = (\tilde{\psi}_0(\mathbf{q}) \pm \tilde{\psi}_1(\mathbf{q})) / \sqrt{2}$ , and the mode operators as  $\hat{c}_{R,L} = (\hat{c}_0 \pm \hat{c}_1) / \sqrt{2}$ . Under this approximation, we can evaluate the density operator  $\hat{n}(\mathbf{q})$  by expanding the field operators  $\hat{\psi}(\mathbf{q})$  and  $\hat{\psi}^\dagger(\mathbf{q})$  in the basis of energy eigenstates, and then truncating the expansion after the first two  $\mathbf{q}$  states. We then express the density operator as

$$\hat{n}(\mathbf{q}) = \sum_{i,j} N_{ij}(\mathbf{q}) \hat{c}_i^\dagger \hat{c}_j \quad (6)$$

$$N(\mathbf{q})_{ij} = \sum_{\mathbf{q}'} \frac{d^3 q'}{(2\pi)^{3/2}} \tilde{\psi}_i^\dagger(\mathbf{q} + \frac{\mathbf{q}'}{2}) R(\mathbf{q} + \frac{\mathbf{q}'}{2}) R(\mathbf{q} - \frac{\mathbf{q}'}{2}) \tilde{\psi}_j(\frac{\mathbf{q}'}{2}) \quad (6)$$

with indices  $i, j \in \{R, L\}$  denoting either the right or left states. Accounting for properties of the right- and left-well states under parity [26], we obtain

$$\hat{n}(\mathbf{q}) = N_{RR}(\mathbf{q}) N + N_{RL}(\mathbf{q}) \hat{c}_R^\dagger \hat{c}_L + N_{RL}(\mathbf{q}) \hat{c}_L^\dagger \hat{c}_R \quad (7)$$

where  $N$  is the total number of atoms in the system. Dropping terms that depend only on  $N$ , one thus finds

$$\hat{H}_{\text{int}} = UN_R \hat{N}_L + \frac{J_1}{2} \hat{C}_R^\dagger \hat{C}_L + \hat{C}_L^\dagger \hat{C}_R + J_2 \hat{C}_R^\dagger \hat{C}_R^\dagger \hat{C}_L \hat{C}_L + \hat{C}_L^\dagger \hat{C}_L^\dagger \hat{C}_R \hat{C}_R \quad (8)$$

where the energies  $U$ ,  $J_1$  and  $J_2$  are given as

$$U = \frac{g}{Z} \int d^3q N_{RL}^2 \quad (9)$$

$$J_1 = 2N \frac{g}{Z} \int d^3q N_{RR}(q) N_{RL}(q) \quad (10)$$

$$J_2 = \frac{g}{2} \int d^3q N_{RL}(q) N_{RL}(-q) \quad (11)$$

Before delving further into the implications of the interaction Hamiltonian given above, let us consider the weak confinement (large  $M$ ) limit at which the right- and left-well states contain no population in the upper ( $\sigma$ ) dressed states, are Gaussian functions well-localized (in  $q$  space) at the right and left potential minima at  $Q=2$ , with rms widths  $\sigma_q = (2M)^{-1/2}$ , and have average density per particle  $\bar{n}_i = \frac{3}{4} = 3/2$ . In calculating the integrals of Eq. 6, we may thus use local values of the rotation matrices  $R(q)$  at  $Q=2$ , as appropriate. We then find

$$U = g \bar{n}_i \sin^2 \frac{Q}{2} \quad (12)$$

$$J_1 = 2N g \bar{n}_i \sin \frac{Q}{2} e^{-\frac{Q^2}{16\sigma_q^2}} \quad (13)$$

$$J_2 = \frac{g}{2} \bar{n}_i \sin^2 \frac{Q}{2} e^{-\frac{Q^2}{4\sigma_q^2}} \quad (14)$$

These approximations can be further simplified by setting  $Q = k$ , and thus  $\sin(Q/2) = \frac{k}{\sqrt{1+k^2}}$ .

Let us presume that the interaction-mediated tunnelling terms  $J_1$  and  $J_2$  are negligibly small. We thus recover the many-body Hamiltonian of Eq. 1 which had applied to the position-space double well. However, examining the interaction energy  $U$ , we now find that the roles of attractive and repulsive interactions are interchanged between the position-space and momentum-space double well treatments: for the case of the momentum-space double-well potential, repulsive interactions ( $g > 0$ ) yield  $U < 0$  and thus are the source of Schrodinger-cat ground states, while attractive interactions ( $g < 0$ ) yield  $U > 0$  and thus are the source of number-squeezed ground states. This opens the door to the production of Schrodinger-cat states for large, robust Bose-Einstein condensates with repulsive interactions through the use of binary collisions as a non-linear coupling.

This reversal of roles for repulsive and attractive interactions in momentum space can be understood in the context of a single-component Bose-Einstein condensate in a harmonic potential. Repulsive interactions lead the

ground-state condensate wavefunction to become larger spatially, thus causing the momentum-space wavefunction to contract (appearing as an attractive interaction in momentum space). Equivalently, one may note that in a Hartree approximation to the many-body state of a Bose-Einstein condensate, the interaction energy is evaluated as an interaction energy density proportional to the square of the density. The density of a Bose gas occupying two distinct momentum states would be spatially modulated by the interference between the momentum states, and, therefore, its interaction energy  $/gn^2$  would be increased (decreased) for the case of repulsive (attractive) interactions. Thus we find repulsive interactions leading to Schrodinger-cat states, a superposition of states in which only one single-particle state is macroscopically occupied, while attractive interactions would lead to a "fractionation" of the condensate between distinct momentum states.

In the system we have described here, the interaction energy  $U$  is a tunable exchange term which, in the case of repulsive interactions, suppresses the superposition of atoms in two distinct momentum states and thereby favors the maximally-entangled state. The exchange term in the interaction Hamiltonian arises from the presence of atoms in identical internal states, but different momentum states. By adjusting the strength of the Rabi coupling, the admixture of internal states  $|A_i\rangle$  and  $|B_i\rangle$  in the right and left well states is varied. For small  $\theta$ , atoms in the right-well state are almost purely in the  $|A_i\rangle$  state, and atoms in the left-well state are almost purely in the  $|B_i\rangle$  state. Thus, the strength of the exchange term is suppressed ( $\sin^2(Q/2) \approx 1$ ), and the product state  $|j_i\rangle / (\hat{C}_R + \hat{C}_L)^N |i\rangle$  remains energetically favored. For larger  $\theta$ , the right and left-well states both contain admixtures of the two internal states; e.g. the right-well state contains atoms in state  $|A_i\rangle$  nearly at rest, while the left-well state contains atoms in state  $|A_i\rangle$  at momentum  $\sim k$ . Significant exchange terms now suppress the product state in favor of the maximally-entangled state.

The dependence of the many-body ground state on the ratio  $U=J$  and the atom number  $N$  has been worked out by various authors [14, 16, 17] for the position-space double-well potential. As we have obtained a Hamiltonian identical in form to the position-space treatment, these predictions would apply directly to our scheme. Significant deviations from the factorized, non-interacting atom solution begin at  $J=J_c \approx 1/N$ ; for repulsive ( $U > 0$ ) or attractive ( $U < 0$ ) interactions this would shift population either away from or towards the state  $|N_L = N/2; N_R = N/2\rangle$ , respectively. Perturbation analysis shows that the many-body state will be well approximated by the Schrodinger-cat state  $(|N; 0\rangle + |0; N\rangle) / \sqrt{2}$  when  $U=J > 1/N$ .

Now returning to Eq. 8, we see that two extra terms appear in  $\hat{H}_{\text{int}}$  which do not conserve the number of particles in the right- and left-well states, representing a form of interaction-mediated tunnelling. The first, involving  $J^{(1)}$ , modifies the tunnelling energy between the right

and left wells. The effect of this term is to reduce the tunnelling rate for repulsive interactions, and increase it for attractive interactions. This can be understood by noting that repulsive interactions tend to raise the energy of the single-particle ground state more than the first excited state since the ground state has a higher density. Our previous analysis of the two-mode approximation accommodates this term by a redefinition of  $J$  as  $J \rightarrow J - J^{(1)}$ , leading to no further complications. The second tunnelling term, involving  $J^{(2)}$ , describes collisions which can redistribute two atoms from the right well to the left well, and vice versa. While this term modifies the conclusions of our simple treatment, we have seen that the magnitudes of both  $J^{(1)}$  and  $J^{(2)}$  are exponentially suppressed with respect to  $U$ , and thus the dominant role of interactions is to create the aforementioned many-body ground states. These terms will, however, play an important role in determining the strength of interactions at which many-body correlations begin to become evident; the scaling of  $J$  (independent of  $g$ ),  $J^{(1)}$ ,  $J^{(2)}$  and  $U$  with the control parameters ( $\lambda$ ,  $g$ ,  $M$ , etc.) are different and thereby provide more tunability to the system.

We performed numerical calculations of the lowest-energy single-particle states to verify the simple scaling behaviour of various terms in the Hamiltonian described above. The single-particle Hamiltonian of Eq. 4 is separable in the three Cartesian coordinates defined so that one axis (say  $\hat{z}$ ) lies along the direction of the Raman momentum transfer  $\mathbf{k}$ . We then have the lowest energy eigenstates as  $\tilde{\psi}_{0,1}(\mathbf{q}) = \tilde{\psi}_{0,1}(q_z) \exp(\frac{q_x^2 + q_y^2}{4}) = 2^{-\frac{1}{2}} \frac{1}{q}$ , a product of harmonic-oscillator ground states in the  $\hat{x}$  and  $\hat{y}$  directions and normalized solutions  $\tilde{\psi}_{0,1}(q_z)$  to the one-dimensional, two-component Schrödinger equation derived from Eq. 4.

These one-dimensional eigenstates, calculated using a restricted basis set of Fourier components over the domain  $-3 \leq q \leq 3$ , are shown in Figure 2 for two different values of the mass parameter  $M$ , and for the condition of exact Raman resonance  $\Delta = 0$  and Rabi frequency  $\sim \hbar E_k = 1=8$ . For weak spatial confinement (large  $M = 50$ ), the lowest two energy eigenstates are indeed nearly entirely composed of lower dressed states ( $(q_z) = 0$ ) and are well-approximated by the sum or difference of Gaussian right- and left-well wavefunctions centered at the potential minima near  $q_z = k = 1=2$ . For stronger spatial confinement (smaller  $M = 8$ ), the enhanced "momentum-space tunnelling" causes the wavefunctions to become less confined in the potential minima. Concurrently, a significant population appears in the upper dressed states.

Parameters which enter into the two-mode Hamiltonian are derived from the numerically-obtained wavefunctions, and are shown in Figure 3. One finds the scaling  $J \propto \exp(-M/4)$  as one expects [27]. The numerical results confirm the scaling behaviour for  $J^{(1)}$  found in the weak confinement (large  $M$ ) limit (Eqs. 12 & 14), but differ slightly from the scaling predicted for  $J^{(2)}$  since

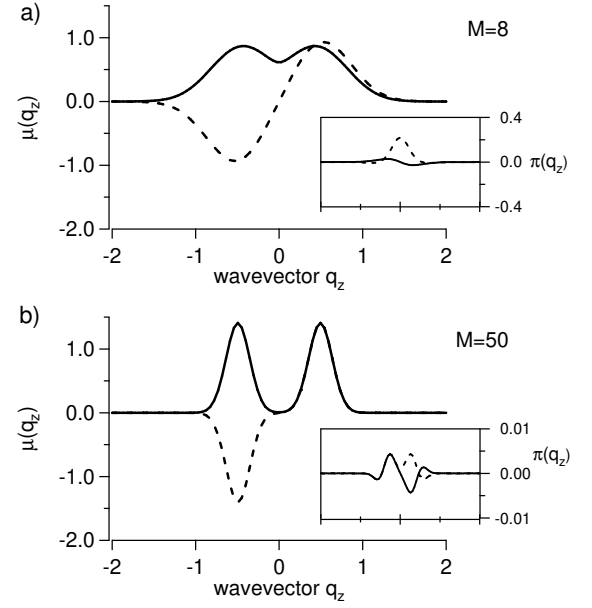


FIG. 2: The two lowest-energy eigenfunctions (solid line for the ground state, dashed for the excited state) which define the right- and left-well modes for the two-mode approximation. Component wavefunctions in the lower ( $q_z$ ) and upper ( $q_z$ ), shown in insets) periodically-dressed states are shown for  $M = 8$  and  $M = 50$ . As the spatial confinement is weakened (larger  $M$ ), the wavefunctions become further localized in the minima of the double-well potential, and the population in the upper dressed state diminishes. Note the different parity of the  $\pi$  components, as discussed in the text. Here  $\sim \hbar E_k = 1=8$ , wavevectors are scaled by  $k$ , and the one-dimensional wavefunctions  $\tilde{\psi}_{0,1}(q_z)$  are shown.

the assumption that the right-well state remains Gaussian in the vicinity of the left-well potential minimum is incorrect. Nevertheless,  $J^{(2)}$  is strongly suppressed for large  $M$ , approximately as  $\exp(-M/3)$ . Also shown is the energy splitting between the second and third lowest eigenenergies; one sees that for weak spatial confinement the lowest two energy eigenstates become well separated from the remaining eigenspectrum, establishing the validity of the two-mode approximation.

Finally, we stress that the two-mode treatment presented here becomes invalid in the Thomas-Fermi regime, where the strength of atomic interactions dominates the zero-point energy in the confining potential. In this situation, additional single-particle states must be considered, resulting in a complicated, self-consistent definition of the right- and left-well states which depends on the number of atoms in these states. How to properly treat such a situation remains an open question, and therefore an important subject for experimental investigation. In related work, Montina and Arcechi [23] obtain right- and left-well states through use of the Gross-Pitaevskii equation, but the validity of their treatment is questionable for systems which are not completely interaction-dominated.

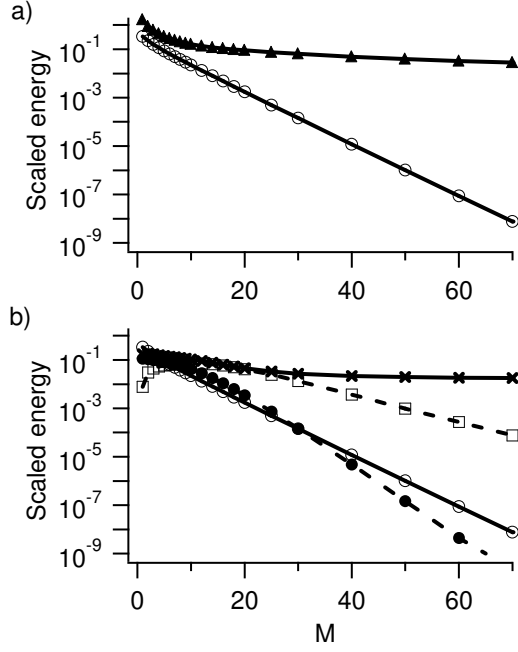


FIG. 3: Numerical calculations of tunnelling and interaction strengths. a) The tunnel splitting  $J$  (open circles, solid line) becomes much smaller than the spacing between the second and third excited states (open triangles, solid line) for moderate values of  $M$ , establishing the validity of the two-mode approximation for weak confinement. b) Tunnelling energies  $J$  (open circles, solid line),  $J^{(1)}$  (open squares, dashed line) and  $J^{(2)}$  (filled circles, dashed line) are suppressed for weaker confinement (exponentially with large  $M$ ), while the strength of the momentum exchange energy  $U$  (X's, solid line) remains large. This provides a route to creating correlated many-body states adiabatically from uncorrelated states by gradually weakening the spatial confinement. The energies in (a) are scaled by  $E_k$ . Dimensionless interaction parameters are plotted as  $U = g\hbar n_i$ ,  $J^{(1)} = 2N g\hbar n_i$ ,  $J^{(2)} = (g\hbar n_i = 2)$ . A Rabi frequency  $\sim \hbar E_k = 1/8$  is chosen.

### III. APPLICATION TO HEISENBERG-LIMITED MEASUREMENT

Several theoretical works have pointed out the potential for correlated many-body states for improving the precision of atomic clocks [4] and interferometers [5, 28], in which phase shifts are measured at the Heisenberg limit  $\propto 1/N$ , rather than the standard quantum limit  $\propto 1/\sqrt{N}$ , where  $N$  is the number of particles used in a single run of the experiment. In particular, Bollinger et al. described the use of the maximally-entangled state in such a measurement [4]. In this section, we point out how dynamical control over experimental parameters can be used fruitfully to generate Schrodinger-cat states suited for the implementation of both Heisenberg-limited spectroscopy and interferometry.

In the system we have described, repulsive interatomic interactions lead to lowest energy many-body states

which are the even- and odd-superposition Schrodinger cat states,  $|\beta_i\rangle = (|j_{Ri}\rangle + |j_{Li}\rangle)/\sqrt{2}$ . The states  $|j_{Ri}\rangle$  and  $|j_{Li}\rangle$  are distinguishable many-body states associated with the right and left potential wells, respectively, which tend toward the limiting cases  $|j_{Ri}\rangle \rightarrow |j; N, i\rangle$  and  $|j_{Li}\rangle \rightarrow |j; N, 0\rangle$  for strong interactions. The energy separation between these two states depends on the residual overlap between  $|j_{Ri}\rangle$  and  $|j_{Li}\rangle$  and the number of atoms in the system (derived, e.g., in Ref. [15]). In the weak-confinement limit  $M \rightarrow 1$ , these right- and left-well states are comprised of the lower dressed states, which are superpositions in both internal and external degrees of freedom. Such a superposition appears to complicate the use of these Schrodinger-cat states for measurement applications.

However, after these Schrodinger-cat states are formed, the dressed right- and left-well states can be converted to pure internal or external states adiabatically, i.e. by modification of experimental parameters on a time-scale which is fast with respect to tunnelling times so as to preserve entanglement, but slow with respect to timescales relevant to the Raman coupling ( $\sim 1/\Omega$ ). If the Rabi frequency  $\Omega$  is adiabatically lowered to zero (the Raman beams are slowly extinguished), atoms in the right-well state would be adiabatically converted to stationary trapped atoms in the  $|\beta_i\rangle$  internal state, while atoms in the left well would be converted to stationary trapped atoms in the  $|\beta_i\rangle$  state. Thus would be prepared a state ideal for Heisenberg-limited measurement of the internal state energy difference  $\sim \hbar \omega_0$ , potentially on a useful hyperfine clock transition. Alternatively, one could adiabatically ramp the detuning from the Raman resonance to large positive or negative values. For example, an adiabatic downward sweep of the frequency difference between the Raman laser beams ( $\sim 1/\Omega$ ) lowers the energy of the  $|\beta_i\rangle$  internal state with respect to the  $|\beta_i\rangle$  internal state in the rotating frame. This adiabatically converts the right- and left-well states to distinguishable momentum states with identical internal states (in this case the  $|\beta_i\rangle$  state). One thereby prepares a state ideal for Heisenberg-limited atomic interferometry.

Furthermore, the timed application of Raman coupling in this system can be used as a "magic beam splitter" [29] to prepare the Schrodinger-cat state dynamically. For simplicity let us make the identification  $|j_{Ri}\rangle = |j; N, i\rangle$  and  $|j_{Li}\rangle = |j; N, 0\rangle$ . Consider a system prepared in the  $|j_i\rangle = |j; N, 0\rangle$  state with no Raman coupling ( $\Omega = 0$ ) { this state corresponds to a zero-temperature Bose-Einstein condensate of  $N$  atoms in the  $|\beta_i\rangle$  internal state. The Raman coupling is then turned on adiabatically, as discussed above. The initial state  $|j_i\rangle$ , being a superposition of the two-lowest energy Schrodinger-cat energy eigenstates, is now led to oscillate coherently, and collectively, between the right- and left-well states. This oscillation is analogous to macroscopic quantum tunnelling observed, for example, in the Rabi oscillations of superconducting qubits [30]. If the Raman coupling is left on for a duration which is  $1/4$  of the Bohr period between the even

and odd Schrodinger-cat states, the many-body state  $|j\rangle$  will evolve as

$$|j\rangle \rightarrow \frac{e^{i\phi} + e^{-i\phi}}{2} |N; 0\rangle + \frac{1 + e^{-i\phi}}{2} |j; N\rangle \quad (15)$$

The Raman beams can be then switched off with the transformation of the state into a momentum-space or internal-state-space Schrodinger-cat state, as desired [1] for a duration  $\tau$ , during which a relative phase can accrue between the two distinguishable portions of the Schrodinger-cat state, i.e.

$$|j\rangle \rightarrow \frac{1}{2} |N; 0\rangle + \frac{1 + e^{iN\tau}}{2} |j; N\rangle \quad (16)$$

Here  $\tau$  is the difference in energy between the single-particle states to which the right- and left-well states are connected when the Raman beams are extinguished. For instance, if we are following the implementation of a measurement of the clock frequency between internal states,  $\tau = \tau_{ij}$ .

Finally, this state must be analyzed. In the scheme of Bollinger et al. [4], a conventional  $\pi/2$  pulse is applied, and a precise measurement is made of the difference between the number of atoms in the  $|A\rangle$  state and the  $|B\rangle$  state. One must establish whether this number difference is even or odd, thus requiring single-atom precision in the number counting.

Ultimately, one may apply a second "magic beam splitter" pulse as before, thus preparing a state

$$|j\rangle \rightarrow \frac{e^{i\phi} - e^{-i\phi}}{2} |N; 0\rangle + \frac{(1 + e^{-i\phi})}{2} |j; N\rangle \quad (17)$$

Measurements on this state would detect all atoms in either the right- or left-well states (say, internal states  $|A\rangle$  or  $|B\rangle$ ), with probabilities which vary periodically with the free-evolution time with frequency  $N$  which is  $N$  times higher than for a single-particle Raman-type mea-

surement. This is the source of the enhanced Heisenberg-level sensitivity. This sensitivity persists even in the presence of overall number fluctuations, presuming that one's goal is to ascertain whether  $\phi = 0$ . However, the correct timing required to yield a perfect "magic beam splitter" will depend on  $N$  [15]. Thus, attaining the highest precision will still require a highly accurate determination of the total atom number  $N$ , though perhaps not necessarily at the single-atom level. A further unexamined issue is how the finite temperature of the atomic sample, which prevents the initial state  $|j\rangle$  from being a pure Bose-Einstein condensate, will impact the precision of these Schrodinger-cat-based measurements.

In conclusion, we have presented an analytic model which identifies the many-body ground states of a weakly-interacting Bose gas which is "periodically dressed" by continuous Raman excitation and confined in an harmonic spatial potential. The system is analyzed in momentum space, wherein the balance between tunnelling and weak interactions dictates whether the ground states are uncorrelated product states of single-particle wavefunctions, or highly correlated states. It is found that interactions in the physical system considered here have the opposite effect as in the dual situation of a position-space double-well potential, that is, repulsive interactions will lead to Schrodinger-cat states while attractive interactions will lead to number-squeezed states with equal numbers of atoms in each well. Further, we show that experimental parameters can be used to dynamically tune the interaction strength and tunnelling rates. This degree of control can be used to generate maximally-entangled states directly suitable for Heisenberg-limited metrology and interferometry.

We thank Lorraine Sadler, Subhadeep Gupta, Joel Moore, and Veronique Savalli for critical discussions and readings. This work was supported by the National Science Foundation under Grant No. 0133999, by the Hellman Faculty Fund, the Sloan Foundation, the Packard Foundation, and the University of California.

- 
- [1] C. H. Bennett et al, *Physical Review Letters* 70, 1895 (1993).
  - [2] C. M. Caves, *Physical Review D* 23, 1693 (1981).
  - [3] D. J. Wineland et al, *Physical Review A* 46, R6797 (1992).
  - [4] J. J. Bollinger et al, *Physical Review A* 54, R4649 (1996).
  - [5] P. Bouyer and M. A. Kasevich, *Physical Review A* 56, R1083 (1997).
  - [6] B. Julsgaard et al, *Nature* 413, 400 (2001).
  - [7] C. A. Sackett et al, *Nature* 404, 256 (2000).
  - [8] M. Brune et al, *Physical Review Letters* 77, 4887 (1996).
  - [9] Y. A. Pashkin et al, *Nature* 421, 823 (2003).
  - [10] A. J. Berkley et al, *Science* 300, 1548 (2003).
  - [11] O. Mandel et al, preprint arXiv:quant-ph/0308080.
  - [12] A. Andre and M. D. Lukin, *Physical Review A* 65, 053819 (2002).
  - [13] A. S. Sorensen and K. Molmer, *Physical Review A* 66, 022314 (2002).
  - [14] A. Imamoglu et al, *Physical Review Letters* 78, 2511 (1997).
  - [15] J. I. Cirac et al, *Physical Review A* 57, 1208 (1998).
  - [16] J. Javanainen and M. Y. Ivanov, *Physical Review A* 60, 2351 (1999).
  - [17] R. W. Spekkens and J. E. Sipe, *Physical Review A* 59, 3868 (1999).
  - [18] C. Ozelet et al, *Science* 291, 2386 (2001).
  - [19] M. G. Reiner et al, *Nature* 415, 39 (2002).
  - [20] C. A. Sackett et al, *Physical Review Letters* 82, 876 (1999).
  - [21] J. Higbie and D. M. Stamper-Kurn, *Physical Review Letters* 88, 090401 (2002).

- [22] D. M. Stamper-Kurn, *New Journal of Physics* 5, 50 (2003).
- [23] A. Montina and F. T. Arecchi, *Physical Review A* 67, 23616 (2003).
- [24] A. J. Leggett, *Reviews of Modern Physics* 73, 307 (2001).
- [25] Such a potential for ultracold alkali atoms might be created by optical trapping at large detunings and/or with linearly polarized light, or by magnetic trapping of two states with identical magnetic moments. For simplicity, we have also chosen a radially-symmetric trap, though our analysis is only slightly modified by trap asymmetry as long as the Raman momentum transfer  $\hbar k$  is aligned along an axis of the trap.
- [26] Defining the operator  $P = P_z$  where  $P$  is the parity operator and  $\sigma_z$  the Pauli matrix, we find for  $\epsilon = 0$  that  $[P, \hat{H}] = 0$ . Given  $\rho_{0,1}^{PD}$  are real, we obtain the relations  $N_{RR}(q) = N_{LL}(q) = N_{RR}(-q)$ , and  $N_{RL}(q) = N_{LR}(-q)$ .
- [27] A similar scalar one-dimensional double-well potential (two offset parabolas connected with a discontinuous slope) is treated analytically as a textbook problem. See for example E. Merzbacher, *Quantum Mechanics*, 2nd Ed. (John Wiley and Sons, New York, 1970), Eq. 5.61.
- [28] M. J. Holland and K. Burnett, *Physical Review Letters* 71, 1355 (1993).
- [29] H. Lee et al., *Journal of Modern Optics* 49, 2325 (2002).
- [30] I. Chiorescu et al., *Science* 299, 1868 (2003).